

Accepted Manuscript

Complexes of zinc(II) with N-[2-(hydroxyalkyliminomethyl)phenyl]-4-methylbenzenesulfonamides: synthesis, structure, photoluminescence properties and biological activity

A.S. Burlov, V.G. Vlasenko, Yu.V. Koshchienko, N.I. Makarova, A.A. Zubenko, Yu.D. Drobin, G.S. Borodkin, A.V. Metelitsa, Ya.V. Zubavichus, D.A. Garnovskii

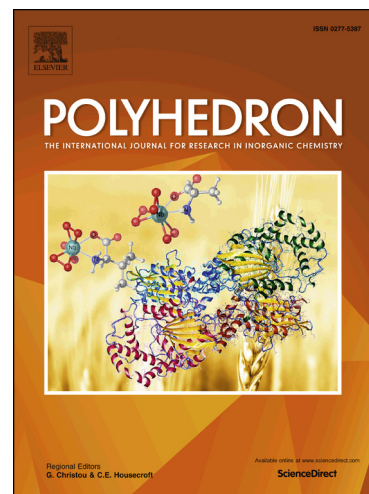
PII: S0277-5387(18)30050-0
DOI: <https://doi.org/10.1016/j.poly.2018.01.020>
Reference: POLY 13018

To appear in: *Polyhedron*

Received Date: 13 November 2017
Accepted Date: 20 January 2018

Please cite this article as: A.S. Burlov, V.G. Vlasenko, Yu.V. Koshchienko, N.I. Makarova, A.A. Zubenko, Yu.D. Drobin, G.S. Borodkin, A.V. Metelitsa, Ya.V. Zubavichus, D.A. Garnovskii, Complexes of zinc(II) with N-[2-(hydroxyalkyliminomethyl)phenyl]-4-methylbenzenesulfonamides: synthesis, structure, photoluminescence properties and biological activity, *Polyhedron* (2018), doi: <https://doi.org/10.1016/j.poly.2018.01.020>

This is a PDF file of an unedited manuscript that has been accepted for publication. As a service to our customers we are providing this early version of the manuscript. The manuscript will undergo copyediting, typesetting, and review of the resulting proof before it is published in its final form. Please note that during the production process errors may be discovered which could affect the content, and all legal disclaimers that apply to the journal pertain.



Complexes of zinc(II) with N-[2-(hydroxyalkyliminomethyl)phenyl]-4-methylbenzenesulfonamides: synthesis, structure, photoluminescence properties and biological activity

A. S. Burlov^a, V. G. Vlasenko^{b,*}, Yu. V. Koshchienko^a, N. I. Makarova^a, A. A. Zubenko^c, Yu. D. Drobin^c, G. S. Borodkin^a, A. V. Metelitsa^a, Ya. V. Zubavichus^d, D. A. Garnovskii^e

^a*Institute of Physical and Organic Chemistry of Southern Federal University, Stachki ave. 194/2, Rostov-on-Don 344090, Russian Federation;*

e-mail: anatoly.burlov@yandex.ru

^b*Institute of Physics of Southern Federal University, Stachki ave. 194, Rostov-on-Don 344090, Russian Federation*

^c*North-Caucasian Zonal Scientific Research Veterinary Institute, Rostov highway, 0, Novocherkassk 346421, Russian Federation*

^d*NRC Kurchatov Institute, 1 Acad. Kurchatov Sq., Moscow 123182, Russian Federation*

^e*Southern Scientific Centre of Russian Academy of Sciences, Chekhova ave. 41, Rostov-on-Don 344006, Russian Federation*

Keywords: Azomethines, Zinc complexes, UV-Vis spectra, Photoluminescence, TD-DFT, Biological activity

ABSTRACT

The synthesis of a series of zinc(II) complexes with Schiff bases products of condensation of 2-tosylammonobenzaldehyde with various aminoalcohols containing aliphatic spacers of a variable length (CH₂)_n (n = 2-6) was performed. All compounds were characterized with C, H, N elemental analysis, FT-IR, ¹H NMR, X-ray absorption spectroscopy, UV-vis and photoluminescence data. The local atomic structures of complexes were determined by X-ray absorption spectroscopy

*Corresponding author

E-mail address: v_vlasenko@rambler.ru

from analysis of EXAFS and XANES of Zn K-edges. The electronic absorption spectra, photoluminescence, and biological activities of the complexes were investigated. The assignments of the experimental UV-vis spectra of zinc(II) complexes have been carried out by Time-Dependent Density Functional Theory TD-DFT calculations.

1. Introduction

Azomethine compounds are versatile molecules with a fortunate combination of structural and chemical properties and have received much attention in research both fundamental and application. Azomethines also constitute a very important class of ligands in coordination chemistry due to their wide applications in the synthesis of a large variety of transition metal complexes with diverse biological activities such as antibacterial, antimicrobial properties [1, 2], exhibit antitumor [3-9] and hypoglycemic [10, 11] activities. For example, water-soluble azomethine derivatives of salicylic aldehyde and amino alcohols (2-aminoethanol and 3-amino-1-propanol) are highly efficient and selective chemical sensors for zinc, which can be used for fluorescent quantification of zinc ions *in vitro* and *in vivo* in various biological objects in the presence of other metal ions [12].

The deliberate introduction of alcoholic groups into the peripheral part of azomethine ligands is a convenient route to polynuclear complexes since a hydroxy group is a versatile O-donor prone to the formation of multi-center bridging bonds [13]. Crystal structures of many coordination compounds with hydroxyethyl (or propyl)salicylaldimine ligands were reported [13-15]. When the alcoholic hydroxyl group is not involved in the coordination, mononuclear structures are formed [14, 15]. Mean while, binuclear structures with bridging oxygen atoms of the aldehyde fragments [13] and even tetrameric structures with bridging oxygen atoms of the alcoholic groups were described [14].

Polynuclear transition metal complexes with azomethines are promising as single-molecule magnets [16, 17] or at least as synthetically affordable models to

study exchange interactions between paramagnetic sites and to verify modern theoretical approaches to the prediction of magnetic properties [18-20].

Complexes of zinc(II) of bi-, three-, and tetradentate azomethinic ligands derived from 2-hydroxy-2-N-tosylaminobenzaldehydes and aliphatic, aromatic, or heterocyclic amines are also efficient metal-containing luminophores. Due to their photo- (PL) and electroluminescent (EL) properties, zinc complexes with azomethinic ligands are a subject of numerous investigations as promising materials for emissive (EML) or conductive (either hole HTL or electron ETL transport) layers in the technology of OLEDs [21-27].

With this regard, the rational synthesis of novel zinc complexes with azomethinic ligands featuring the coordination node ZnN_4 and manifesting EL properties and bioactivity is an important and urgent problem of contemporary coordination chemistry.

The present paper is devoted to the synthesis of zinc complexes with azomethinic ligands of the N-[2-(hydroxyalkyliminomethyl)phenyl]-4-methylbenzenesulfonamide family, which bear a terminal hydroxyl function separated from the imine group by an aliphatic spacer of a variable length $(CH_2)_n$ ($n=2-6$). The presence of such a long and flexible spacer hinders the involvement of the OH group in metal binding and favors the formation of the monomeric structure with the ZnN_4 core. Molecular structures, PL, and biological properties of the synthesized complexes were studied. To the best of our knowledge, no closely related substances have been described so far.

2. Experimental

2.1. Materials required and general methods

All solvents, zinc acetate dihydrate, 2-amino-1-ethanol, 3-amino-1-propanol, 4-amino-1-butanol, 5-amino-1-pentanol, 6-amino-1-hexanol were purchased from Alfa Aesar and used as received.

C, H, N elemental analyses were carried out on a Carlo Erba TCM 480 apparatus using sulfanilamide as a reference. The metal content was determined gravimetrically in the analytical laboratory of the Institute of Physical and Organic Chemistry (SFU, Rostov-on-Don, Russia). Melting points were measured on a Kofler table.

Infrared spectra were recorded on a Varian Excalibur-3100 FT-IR spectrophotometer for powders of compounds **1a**, **2a-e** and solution-cast films of free azomethine ligands **1b-e**.

¹H NMR spectra were measured on a Bruker Avance-600 (600 MHz) spectrometer at ambient temperature in DMSO-d₆ with the signal of residual 2H of the solvent as the internal reference.

UV-vis spectra were registered on «Varian Cary 100» spectrophotometer. Photoluminescent spectra were measured on a «Varian Cary Eclipse» fluorescence spectrophotometer. DMSO of the spectrally pure grade from Sigma-Aldrich was used as a solvent. All UV-vis and fluorescence spectra were recorded using standard quartz cells with an optical path of 1 cm at room temperature at $c = 4.0 \cdot 10^{-5}$ M. Fluorescence quantum yields were determined using the method by Parker-Rice [28] with a solution of quinine bisulfate in 0.1 N H₂SO₄ ($\phi = 0.52$, $\lambda_{\text{ex}} = 365$ nm) as a standard luminophore [29].

2.2. Synthesis of free ligands

2.2.1. The general method for the synthesis of *N*-[2-(hydroxyalkyliminomethyl)phenyl]-4-methylbenzenesulfonamides (**1a-e**)

A solution containing 2 mmol of respective amino alcohol (0.12 g of 2-amino-1-ethanol for **1a**, 0.15 g of 3-amino-1-propanol for **1b**, 0.18 g of 4-amino-1-butanol for **1c**, 0.21 g of 5-amino-1-pentanol for **1d**, or 0.23 g of 6-amino-1-hexanol for **1e**) in 5 mL of methanol was added to a solution of 0.55 g (2 mmol) of 2-(*N*-tosylamino)benzaldehyde in 10 mL of benzene. The mixture was refluxed during 1 h. After that the solvent was distilled off on a rotary evaporator to dryness.

Safety. Benzene is a highly flammable and very toxic solvent. (**Caution:** chronic toxicity, carcinogenicity, mutagenicity). Avoid breathing vapor and contact with skin. Protective clothing and fume hood are required working in laboratory.

2.2.2. *N*-[2-[(*Z*)-2-Hydroxyethyliminomethyl]phenyl]-4-methylbenzenesulfonamide
(1a)

Yellow crystals, m.p. = 58-59 °C. Yield 0.61 g, 96%. Anal. Calc. for C₁₆H₁₈N₂O₃S: C, 60.36; H, 5.70; N, 8.80. Found: C, 60.43; H, 5.78; N, 8.84%. IR spectrum, selected bands, cm⁻¹: 3321 ν (OH), 1651 ν (CH=N), 1337 ν_{as} (SO₂), 1125, 1069 ν_{s} (SO₂). ¹H NMR, δ (ppm): 2.29 (s, 3H, CH₃), 3.66-3.70 (m, 4H, CH₂), 4.76 (s, 1H, OH), 7.03-7.06 (m, 1H, C_{Ar}-H), 7.27-7.34 (m, 3H, C_{Ar}-H), 7.44-7.48 (m, 2H, C_{Ar}-H), 7.66 (dd, 2H, ³J = 6.6 Hz, ⁴J = 1.8 Hz, C_{Ar}-H), 8.42 (s, 1H, CH=N), 12.74 (br.s, 1H, NH).

2.2.3. *N*-[2-[(*Z*)-3-Hydroxypropyliminomethyl]phenyl]-4-methylbenzenesulfonamide
(1b)

Yellow oil. Yield 0.62 g, 93%. Anal. Calc. for C₁₇H₂₀N₂O₃S: C, 61.42; H, 6.06; N, 8.43. Found: C, 61.33; H, 6.14; N, 8.53%. IR spectrum, selected bands, cm⁻¹: 3410 ν (OH), 1650 ν (CH=N), 1336 ν_{as} (SO₂), 1159 ν_{s} (SO₂). ¹H NMR, δ (ppm): 1.80 (q, 2H, ³J = 6.6 Hz, CH₂), 2.29 (s, 3H, CH₃), 3.52 (br.s, 2H, CH₂), 3.64-3.66 (m, 2H, CH₂), 4.52 (s, 1H, OH), 7.05 (t, 1H, ³J = 7.5 Hz, C_{Ar}-H), 7.29-7.35 (m, 3H, C_{Ar}-H), 7.46 (dd, 2H, ³J = 7.8 Hz, ⁴J = 1.8 Hz, C_{Ar}-H), 7.62 (dd, 2H, ³J = 6.6 Hz, ⁴J = 1.8 Hz, C_{Ar}-H), 8.45 (s, 1H, CH=N), 13.22 (br.s, 1H, NH).

2.2.4. *N*-[2-[(*Z*)-4-Hydroxybutyliminomethyl]phenyl]-4-methylbenzenesulfonamide
(1c)

Yellow oil. Yield 0.63 g, 91%. Anal. Calc. for C₁₈H₂₂N₂O₃S: C, 62.40; H, 6.40; N, 8.09. Found: C, 62.48; H, 6.34; N, 8.14%. IR spectrum, selected bands, cm⁻¹: 3423 ν (OH), 1633 ν (CH=N), 1336 ν_{as} (SO₂), 1155 ν_{s} (SO₂). ¹H NMR, δ (ppm): 1.52-1.55 (m, 2H, CH₂), 1.69-1.71 (m, 2H, CH₂), 2.28 (s, 3H, CH₃), 3.49 (q, 2H, ³J = 4.8 Hz,

CH₂), 3.60-3.63 (m, 2H, CH₂), 4.47 (br.s, 1H, OH), 7.06 (t, 1H, ³J = 7.5 Hz, C_{Ar}-H), 7.30 (t, 2H, ³J = 8.6 Hz, C_{Ar}-H), 7.32-7.36 (m, 1H, C_{Ar}-H), 7.46 (dd, 1H, ³J = 7.6 Hz, ⁴J = 1.5 Hz, C_{Ar}-H), 7.50 (d, 1H, ³J = 8.3 Hz, C_{Ar}-H), 7.64-7.66 (m, 2H, C_{Ar}-H), 8.45 (s, 1H, CH=N), 13.35 (s, 1H, NH).

2.2.5. *N*-[2-[(*Z*)-5-Hydroxypentyliminomethyl]phenyl]-4-methylbenzenesulfonamide (**1d**)

Yellow oil. Yield 0.66 g, 92%. Anal. Calc. for C₁₉H₂₄N₂O₃S: C, 63.31; H, 6.71; N, 7.77. Found: C, 63.33; H, 6.80; N, 7.74%. IR spectrum, selected bands, cm⁻¹: 3409 ν(OH), 1633 ν(CH=N), 1338 ν_{as}(SO₂), 1155, 1164 ν_s(SO₂). ¹H NMR, δ (ppm): 1.40-1.42 (m, 2H, CH₂), 1.46-1.50 (m, 2H, CH₂), 1.64 (q, 2H, ³J = 7.3 Hz, CH₂), 2.29 (s, 3H, CH₃), 3.40-3.42 (m, 2H, CH₂), 3.58-3.60 (m, 2H, CH₂), 4.35 (s, 1H, OH), 7.03-7.06 (m, 1H, C_{Ar}-H), 7.29-7.35 (m, 3H, C_{Ar}-H), 7.45-7.47 (m, 2H, C_{Ar}-H), 7.61-7.63 (m, 2H, C_{Ar}-H), 8.45 (s, 1H, CH=N), 13.16 (br.s, 1H, NH).

2.2.6. *N*-[2-[(*Z*)-6-Hydroxyhexyliminomethyl]phenyl]-4-methylbenzenesulfonamide (**1e**)

Yellow oil. Yield 0.69 g, 92%. Anal. Calc. for C₂₀H₂₆N₂O₃S: C, 64.14; H, 7.00; N, 7.48. Found: C, 64.23; H, 7.08; N, 7.54%. IR spectrum, selected bands, cm⁻¹: 3408 ν(OH), 1634 ν(CH=N), 1337 ν_{as}(SO₂), 1157, 1167 ν_s(SO₂). ¹H NMR, δ (ppm): 1.36-1.45 (m, 6H, CH₂), 1.63 (q, 2H, ³J = 7.7 Hz, CH₂), 2.29 (s, 3H, CH₃), 3.39 (br.s, 2H, CH₂), 3.58-3.60 (m, 2H, CH₂), 4.31 (s, 1H, OH), 7.04-7.06 (m, 1H, C_{Ar}-H), 7.29-7.35 (m, 3H, C_{Ar}-H), 7.45-7.47 (m, 2H, C_{Ar}-H), 7.61 (s, 2H, C_{Ar}-H), 8.45 (s, 1H, CH=N), 13.27 (br.s, 1H, NH).

2.3. Synthesis of complexes

2.3.1. The general procedure for the preparation of complexes **2a-e**

A solution containing 2 mmol of appropriate amino alcohol (0.12 g of 2-amino-1-ethanol for **2a**, 0.15 g of 3-amino-1-propanol for **2b**, 0.18 g of 4-amino-1-

butanol for **2c**, 0.21 g of 5-amino-1-pentanol for **2d**, 0.23 g of 6-amino-1-hexanol for **2e**) in 10 mL of acetonitrile was added to a solution of 0.55 g (2 mmol) of 2-(N-tosylamino)benzaldehyde in 20 mL of acetonitrile. The solution was refluxed during 1 h and then a hot solution of 0.22 g (1 mmol) of zinc acetate dihydrate in 10 mL of methanol was added and the reaction mixture was refluxed again for 1 h. After cooling to r.t., the precipitates of complexes formed (**2a-e**) were filtered off, washed twice with hot methanol (10 mL) and dried in *vacuo*. All products were crystallized from a dichloromethane-methanol 1:2 mixture.

2.3.2. *Bis*{*N*-[2-[(*Z*)-2-hydroxyethyliminomethyl]phenyl]-4-methylbenzenesulfonamide}zinc(II) (**2a**)

Colorless crystals, m.p. > 260 °C. Yield 0.53 g, 75%. Anal. Calc. for $C_{32}H_{34}N_4O_6S_2Zn$: C, 54.89; H, 4.89; N, 8.00; Zn, 9.34. Found: C, 54.90; H, 4.95; N, 8.12; Zn, 9.45 %. IR spectrum, selected bands, cm^{-1} : 3305 $\nu(OH)$, 1628 $\nu(CH=N)$, 1288 $\nu_{as}(SO_2)$, 1135 $\nu_s(SO_2)$. 1H NMR, δ (ppm): 2.24 (s, 6H, CH_3), 3.45 (br.s, 2H, CH_2), 3.54 (br.s, 4H, CH_2), 4.12 (br.s, 2H, CH_2), 5.00 (t, 2H, $^3J = 5.4$ Hz, OH), 6.86 (t, 2H, $^3J = 7.9$ Hz, C_{Ar-H}), 7.14 (d, 4H, $^3J = 8.3$ Hz, C_{Ar-H}), 7.19-7.22 (m, 2H, C_{Ar-H}), 7.27 (d, 2H, $^3J = 7.9$ Hz, C_{Ar-H}), 7.50-7.52 (m, 2H, C_{Ar-H}), 7.92 (d, 4H, $^3J = 8.3$ Hz, C_{Ar-H}), 8.50 (s, 2H, $CH=N$).

2.3.3. *Bis*{*N*-[2-[(*Z*)-3-hydroxypropyliminomethyl]phenyl]-4-methylbenzenesulfonamide}zinc(II) (**2b**)

Colorless crystals, m.p. > 260 °C. Yield 0.62 g, 85%. Anal. Calc. for $C_{34}H_{38}N_4O_6S_2Zn$: C, 56.08; H, 5.26; N, 7.69; Zn, 8.98. Found: C, 56.18; H, 5.31; N, 7.72; Zn, 9.01%. IR spectrum, selected bands, cm^{-1} : 3356 $\nu(OH)$, 1628 $\nu(CH=N)$, 1288 $\nu_{as}(SO_2)$, 1136 $\nu_s(SO_2)$. 1H NMR, δ (ppm): 1.68 (br.s, 4H, CH_2), 2.24 (s, 6H, CH_3), 3.26-3.29 (m, 4H, CH_2), 3.60 (br.s, 2H, CH_2), 4.00 (br.s, 2H, CH_2), 4.46 (t, 2H, $^3J = 5.0$ Hz, OH), 6.86 (t, 2H, $^3J = 7.9$ Hz, C_{Ar-H}), 7.13 (d, 4H, $^3J = 8.2$ Hz, C_{Ar-H}), 7.19-7.22 (m, 2H, C_{Ar-H}), 7.27 (d, 2H, $^3J = 8.5$ Hz, C_{Ar-H}), 7.50 (dd, 2H, $^3J = 7.8$ Hz, $^4J = 1.7$ Hz, C_{Ar-H}), 7.88 (d, 4H, $^3J = 8.3$ Hz, C_{Ar-H}), 8.55 (s, 2H, $CH=N$).

2.3.4. *Bis{N-[2-[(Z)-4-hydroxybutyliminomethyl]phenyl]-4-methylbenzenesulfonamide}zinc(II) (2c)*

Colorless crystals, m.p. > 260 °C. Yield 0.57 g, 75%. Anal. Calc. for C₃₆H₄₂N₄O₆S₂Zn: C, 57.17; H, 5.60; N, 7.41; Zn, 8.65. Found: C, 57.10; H, 5.65; N, 7.38; Zn, 8.71%. IR spectrum, selected bands, cm⁻¹: 3339 ν(OH), 1633 ν(CH=N), 1288 ν_{as}(SO₂), 1135 ν_s(SO₂). ¹H NMR, δ (ppm): 1.22-1.27 (m, 4H, CH₂), 1.45-1.50 (m, 4H, CH₂), 2.24 (s, 6H, CH₃), 3.08-3.18 (m, 4H, CH₂), 3.40-3.47 (m, 2H, CH₂), 4.04 (br.s, 2H, CH₂), 4.25 (s, 2H, OH), 6.86 (t, 2H, ³J = 7.4 Hz, C_{Ar}-H), 7.15 (d, 4H, ³J = 8.0 Hz, C_{Ar}-H), 7.19-7.23 (m, 2H, C_{Ar}-H), 7.33 (d, 2H, ³J = 8.6 Hz, C_{Ar}-H), 7.49 (dd, 2H, ³J = 7.9 Hz, ⁴J = 1.7 Hz, C_{Ar}-H), 7.92 (d, 4H, ³J = 8.3 Hz, C_{Ar}-H), 8.54 (s, 2H, CH=N).

2.3.5. *Bis{N-[2-[(Z)-5-hydroxypentyliminomethyl]phenyl]-4-methylbenzenesulfonamide}zinc(II) (2d)*

Colorless crystals, m.p. > 260 °C. Yield 0.59 g, 75%. Anal. Calc. for C₃₈H₄₆N₄O₆S₂Zn: C, 58.19; H, 5.91; N, 7.14; Zn, 8.34. Found: C, 58.29; H, 6.00; N, 7.28; Zn, 8.42%. IR spectrum, selected bands, cm⁻¹: 3352 ν(OH), 1633 ν(CH=N), 1296 ν_{as}(SO₂), 1135 ν_s(SO₂). ¹H NMR, δ (ppm): 1.06-1.14 (m, 8H, CH₂), 1.43 (br.s, 4H, CH₂), 2.24 (s, 6H, CH₃), 3.17 (q, 4H, ³J = 5.8 Hz, CH₂), 3.40-3.45 (m, 2H, CH₂), 4.08 (br.s, 2H, CH₂), 4.20 (t, 2H, ³J = 5.1 Hz, OH), 6.86 (t, 2H, ³J = 7.0 Hz, C_{Ar}-H), 7.16 (d, 4H, ³J = 8.6 Hz, C_{Ar}-H), 7.20-7.23 (m, 2H, C_{Ar}-H), 7.34 (d, 2H, ³J = 8.5 Hz, C_{Ar}-H), 7.49 (dd, 2H, ³J = 7.9 Hz, ⁴J = 1.8 Hz, C_{Ar}-H), 7.94 (d, 4H, ³J = 8.3 Hz, C_{Ar}-H), 8.54 (s, 2H, CH=N).

2.3.6. *Bis{N-[2-[(Z)-6-hydroxyhexyliminomethyl]phenyl]-4-methylbenzenesulfonamide}zinc(II) (2e)*

Colorless crystals, m.p. > 260 °C. Yield 0.63 g, 78%. Anal. Calc. for C₄₀H₅₀N₄O₆S₂Zn: C, 59.13; H, 6.20; N, 6.90; Zn, 8.05. Found: C, 59.20; H, 6.26; N, 6.95; Zn, 8.17%. IR spectrum, selected bands, cm⁻¹: 3361 ν(OH), 1633 ν(CH=N),

1296 $\nu_{\text{as}}(\text{SO}_2)$, 1136 $\nu_{\text{s}}(\text{SO}_2)$. ^1H NMR, δ (ppm): 0.98-1.04 (m, 8H, CH_2), 1.11-1.17 (m, 4H, CH_2), 1.38-1.44 (m, 4H, CH_2), 2.25 (s, 6H, CH_3), 3.19-3.23 (m, 4H, CH_2), 3.41-3.45 (m, 2H, CH_2), 4.10 (br.s, 2H, CH_2), 4.20 (t, 2H, $^3\text{J} = 5.2$ Hz, OH), 6.85-6.87 (m, 2H, $\text{C}_{\text{Ar}}\text{-H}$), 7.16 (d, 4H, $^3\text{J} = 8.0$ Hz, $\text{C}_{\text{Ar}}\text{-H}$), 7.21-7.24 (m, 2H, $\text{C}_{\text{Ar}}\text{-H}$), 7.36 (d, 2H, $^3\text{J} = 8.3$ Hz, $\text{C}_{\text{Ar}}\text{-H}$), 7.48 (dd, 2H, $^3\text{J} = 7.9$ Hz, $^4\text{J} = 1.7$ Hz, $\text{C}_{\text{Ar}}\text{-H}$), 7.95 (d, 4H, $^3\text{J} = 8.3$ Hz, $\text{C}_{\text{Ar}}\text{-H}$), 8.55 (s, 2H, $\text{CH}=\text{N}$).

2.4. X-ray absorption spectroscopy

Zn *K*-edge EXAFS spectra for the complexes were recorded at the "Structural Materials Science" beamline of the Kurchatov Synchrotron Radiation Source (Moscow, Russia) [30] with the storage ring operating at electron energy of 2.5 GeV and current of 80–100 mA. A Si(111) channel-cut monochromator was used for the energy selection. All data were measured in the transmission mode. Sample thicknesses corresponded to an absorption jump $\Delta\mu_{\text{x}}=0.5\text{--}1.0$.

EXAFS data ($\chi_{\text{exp}}(k)$) were analyzed using the IFEFFIT data analysis package [31]. EXAFS data reduction used standard procedures for the pre-edge subtraction and spline background removal. The radial pair distribution functions around the Zn ions were obtained by the Fourier transformation (FT) of the k^3 -weighted absorption function $\chi_{\text{exp}}(k)$ range of photoelectron wave numbers $k = 2.4\text{--}13.0 \text{ \AA}^{-1}$. Structural parameters including interatomic distances (R_i), coordination numbers (N_i) and distance RMS deviations due to the thermal motion and disorder-induced static deviations of atomic positions, also known as Debye–Waller factors (σ^2) were found by non-linear fitting of the theoretical spectra against the experimental ones.

$$\chi(k) = S_0^2 \sum_{i=1}^n \frac{N_i}{R_i^2} \frac{F_i(k)}{k} e^{-\frac{2R_i}{\lambda(k)}} e^{-2\sigma_i^2 k^2} \sin(2kR_i + \Psi_i(k)), \quad (1)$$

The experimental data were simulated using theoretical photoelectron mean-free-path (λ), photoelectron backscattering amplitude $F_i(k)$ and phase functions (formula 1) calculated using the FEFF7 program [32]. The amplitude reduction factor due to extrinsic losses S_0^2 and the edge energy shift E_0 were calibrated by fitting EXAFS data for spectra of reference compounds with known crystal

structures. The amplitude reductions factors S_0^2 were found to be equal to 0.9 in all cases.

The accuracy of the fits was estimated by the standard mean-square deviation criterion (formula 2) (Q -factor),

$$Q^2 = \frac{\sum_{i=1}^m w(k_i) [k_i \chi_{\text{exp}}(k_i) - k_i \chi_{\text{th}}(k_i)]^2}{\sum_{i=1}^m w(k_i) [k_i \chi_{\text{exp}}(k_i)]^2} \quad (2)$$

where $w(k_i)$ is a weighting function, m is the number of experimental points.

2.5. Quantum-chemical calculations

The GAUSSIAN-03 program package [33] was used for DFT calculations. Ground-state geometry of isolated molecules of the complexes under study was optimized using the Becke's three-parameter exchange functional [34], Lee–Yang–Parr correlation functional (B3LYP) [35] and standard split-valence polarized 6-31G(d) basis set [36, 37]. The absence of imaginary frequencies in the normal mode analysis ensured optimized geometry to be the true energy minimum, not a transition state.

The simulation of UV-vis absorption spectra for these complexes was performed within the Time-Dependent Density Functional Theory (TD-DFT) formalism using the optimized geometry subject to solvent effects as predicted by the standard polarizable continuum model (PCM) [38].

2.6. Antimicrobial activity assay

Antimicrobial properties of azomethines **1a-e** and complexes **2a-e** were studied by means of two-fold serial dilutions in a liquid nutrient medium [39, 40]. Suspensions of bacterial cultures (2 mL) with a concentration of $5.0 \cdot 10^5$ microbial cells per mL were mixed with equal amount of test substance solutions at variable concentrations in special vials (which gave rise to a nominal two-fold decrease in the bacteria concentration to $2.5 \cdot 10^5$ per mL). Vials were kept in an incubator for

18 h at 37 °C. In parallel, vials containing nutrient medium and bacteria at a concentration of $2.5 \cdot 10^5$ per mL and only nutrient medium without bacteria were incubated under identical conditions as positive control and negative control probes, respectively. Standard strains of bacteria *Staphylococcus aureus* P-209 and *Escherichia coli* 078 (field isolates from the collection of the Rostov regional veterinary laboratory) were used for the antimicrobial activity tests. Activity of the azomethines and zinc complexes was compared with that of a commercial antibiotic sulfadimethoxine (chemically pure grade).

2.7. Antiprotozoal activity assay

Antiprotozoal activity was studied against infusoria *Colpoda steinii* (field isolate from the collection of the laboratory of parasitology of the North-Caucasian Zonal Scientific-Research Veterinary Institute, Russia) using a method described elsewhere [41]. The tests were carried out in a 96-well microplate typically used for the enzyme-linked immunosorbent assays (ELISA), 12 wells of the first row were used. A 1:1 mixture of boiled tap and sterile distilled water was used as a medium. Initially the substance being tested was dissolved in distilled water. Serial dilutions of the test solutions were prepared as follows:

Solution No.1: 5 mg of the substance under study was dissolved in 50 μ L of 70% aqueous DMSO under stirring, then 5 mL of distilled water was carefully added to give an apparent concentration of the probe 1000 μ g/mL, 150 μ L of the prepared solution was placed into the well No.1 of the microplate.

Solutions No.2-12: 150 μ L of 1:1 mixture of boiled tap and sterile distilled water was placed into the wells No.2-12 of the microplate using an automated 8-channel pipette. Then 150 μ L of the solution No.1 was placed into the well No.2 under stirring. After complete mixing an aliquot of 150 μ L of solution No.2 was placed into the well No.3. A similar procedure was applied to all further wells. In order to provide identical volumes of solutions in all the wells, 150 μ L of the solution was removed from the last well No.12. Aliquots of the *Colpoda steinii* protozoa culture suspended in water preliminary incubated for 3 days (30 μ L) were

added to all wells in such a way that no less than 10-15 active infusoria were distinctly visible in the field-of-view of an optical microscope. The microplate was covered with a lid and left at room temperature (20-22 °C) for 18-20 h.

Test results were controlled as follows: 30 µL of content of each well one-by-one starting from the well No.12 was transferred onto a clean glass slide and examined under an optical microscope at a magnification of 10×15 to check for the presence of living protozoa. The minimum protistocidal concentration of a substance under study corresponded to the first well encountered with no living infusoria. In a similar way, the following control solutions were tested:

- blank medium (boiled water + distilled water) – 5 wells;
- DMSO (50 µL of 70% DMSO + 5 mL of distilled water serially diluted exactly as in the case of the tested substances) – 12 wells;
- commercial antiprotozoal agent toltrazuril (2.5% solution serially diluted similarly to the tested substances).

2.8. *Fungistatic activity assay*

Antifungal activity of the compounds was determined by the agar-diffusion method according to the guideline [42] for fungi culture *Penicillium italicum* Wehmer (1894) (field isolate, from the collection of micromycetes of the laboratory of mycotoxicology of the North-Caucasian Zonal Scientific Research Veterinary Institute, Russia). A commercial fungicide fundazol was used for comparison. An aqueous solution of fundazol was placed on a disc of filter paper (ND-PMP-1 Paster Central Research Institute of Epidemiology and Microbiology) in an amount of 15 µg per disc with a diameter of 8 mm.

3. Results and discussion

3.1. *Synthesis and spectroscopic properties of azomethines as free ligands and their derived zinc complexes*

According to the elemental analysis, all complexes have are characterized by the ZnL_2 composition. In the IR spectra of complexes **2a-e**, a broad vibration band in the region of $3305-3361\text{ cm}^{-1}$ $\nu(\text{OH})$ is preserved, but its intensity is reduced as compared to that in the respective free ligands **1a-e**. The stretching vibration band $\nu(\text{CH}=\text{N})$ redshifts with respect to the free ligands to $1628-1634\text{ cm}^{-1}$. Similarly, the asymmetric and symmetric stretching vibrations of the SO_2 group redshift by 50 cm^{-1} . In the ^1H NMR spectra of complexes **2a-e**, the signal of the tosylamino proton (observed as a singlet at $12.74-13.35\text{ ppm}$ in free ligands) disappear, whereas that of the imine proton ($\text{CH}=\text{N}$) shifts downfield to $\delta\ 8.52 - 8.56\text{ ppm}$ (instead of $8.42-8.45\text{ ppm}$). The signal of the OH proton is preserved and appears at $4.20-5.00\text{ ppm}$.

Such spectral observations of IR and ^1H NMR spectra are indicative of the formation of complexes with the $\{\text{ZnN}_4\}$ coordination core and ZnL_2 stoichiometry, in which the azomethines act as bidentate chelate monoanionic ligands, and the terminal hydroxyl group remains uncoordinated [23, 25, 43-47].

3.2. The X-ray absorption spectroscopy

Parameters of the local atomic structure of complexes **2a-e** were determined from the analysis of Zn *K*-edge EXAFS and XANES spectra. Figure **1a** (left panel) shows normalized XANES spectra and their first derivatives $d\mu/dE$. For all complexes **2a-e**, the shapes of XANES spectra are similar and are characterized by the absence of pre-edge peaks and intense features just above the absorption edges. The pre-edge peak in XANES is caused mainly by quadrupole electronic transitions $1s \rightarrow 3d$ involving atomic orbitals of the central metal atoms, which are formally forbidden by the dipole selection rules. These peaks can gain some intensity to be registered in spectra for low-symmetry coordination polyhedra of the metal ion due to partial $4p-3d$ hybridization. But these arguments are not applicable to Zn(II) derivatives, since it has a completely filled $3d$ -shell. First derivatives $d\mu/dE$ of Zn *K*-edge absorption spectra for complexes **2a-e** show a broad main maximum with a complicated multiple-component structure due to the splitting of Zn $4p^*$ -orbitals in

an asymmetric ligand field. A comparison of experimental XANES spectra with those reported in the literature [48-50] implies the tetrahedral environment of zinc ions in the complexes.

Quantitative characteristics of the nearest atomic environment of zinc ions in the complexes **2a-e** were obtained from the analysis of EXAFS spectra. MFT $k^3\chi(k)$ for complexes **2a-e** are shown in Fig. 1b (right panel) and the best-fit parameters of the local structure are listed in Table 1.

Figure 1.

For all compounds **2a-e**, MFTs show a main peak at $r = 1.63 \text{ \AA}$ due to the photoelectron scattering on the first coordination sphere (CS), and much weaker peaks of more distant coordination spheres.

The initial structural model of zinc environment in complexes **2a-e** was constructed using crystallographic data for similar complexes retrieved from the Cambridge Structural Database. According to the non-linear fitting of EXAFS, the first CS of Zn ions for all complexes consists of four N atoms at an average distance of 2.03 \AA (Table 1). The best-fit values of Debye-Waller factors ($0.0031\text{-}0.0035 \text{ \AA}^2$) for the first CS Zn-N are typical values for spectra of such complexes measured at room temperature [48-50].

Table 1.

Thus Zn *K*-edge EXAFS and XANES data for the complexes **2a-e** fully support the suggestion of ZnL_2 composition with only tosylamino and imine nitrogen atoms involved into the coordination with Zn and hydroxy groups of $\text{OH}(\text{CH}_2)_n$ spacers ($n = 2\text{-}6$) remaining intact regardless of their length.

3.3. Electronic absorption spectra and photoluminescence of the zinc complexes

A comparative study of UV-vis and PL properties of the zinc complexes **2a-e** were performed at room temperature in DMSO solutions. The electronic absorption spectra of **2a-e** are shown in Fig. 2, essential optical characteristics are summarized in Table. 2.

Table 2.

Figure 2.

UV-vis spectra of the complexes **2a-e** in the spectral range from 265 to 400 nm are virtually identical along the whole series and show two main absorption bands centered at 350 nm ($\epsilon = 11540\text{-}12890 \text{ M}^{-1} \text{ cm}^{-1}$) and 270 nm ($\epsilon = 21700\text{-}25300 \text{ M}^{-1} \text{ cm}^{-1}$) with slightly different relative intensities (Table 2, Fig. 2). All complexes **2a-e** demonstrate bright blue fluorescence (Table 2, Fig. 3).

Figure 3.

Fluorescence maxima and fluorescence quantum yields fall into narrow ranges $\lambda_{\text{max}} = 428 - 430 \text{ nm}$ and $\phi = 0.32\text{-}0.35$, respectively, for all complexes **2a-e** (Table 2). The fluorescence excitation spectra of **2a-e** fit well their absorption spectra, indicating that their fluorescence was correctly assigned zinc complexes ZnL_2 . (Table 2, Figure 4).

Figure 4.

The above data show that the optical properties of the complexes **2a-e** are formed by the coordination core that is common for all of them and are essentially independent of the length of the $(\text{CH}_2)_n$ spacer within the N-hydroxyalkyl substituent.

Thus, the novel zinc complexes **2a-e** shows highly efficient PL properties in the blue spectral region, which makes them promising luminophores for the fabrication of white-light OLEDs.

3.4. Interpretation of UV-vis spectra based on TD-DFT calculations

In order to assign bands observed in the experimental UV-vis spectra to specific singlet-singlet electronic transitions spectral simulation within the TD-DFT formalism was utilized. Theoretical calculations predicted very similar values of electronic transition characteristics for all zinc complexes **2a-e** indicating again that the hydroxyalkyl radicals do not participate in the charge transfer processes reflected in UV-vis spectra. Therefore, results of calculations are presented below only for **2a**, for other complexes the respective data can be found in Supplementary Materials (Table S1-S5, Fig. S1-S5).

The theoretical UV-vis spectrum for **2a** corresponds well to the experimental one, as shown in Fig. 4. Energies (E), wavelengths (λ_{cal}), oscillator strengths (f), and frontier molecular orbitals (FMO) involved for all important singlet-singlet electronic transitions are compiled in Table 3. The theoretical spectrum was constructed as a convolution of Gaussian peaks associated with each of the electronic transitions taking into account their positions and oscillator strengths.

The long-wavelength part of the experimental UV-vis spectrum is formed by a wide absorption band with a maximum at 353 nm. As expected for Zn(II) complexes with the completely filled d-shell and further confirmed by the calculation, no d-d intra shell transitions of Zn is involved. Instead, according to the TD-DFT spectral simulations, the absorption maximum at 353 nm is formed by a superposition of four transitions, viz., HOMO→LUMO, HOMO→LUMO+1, HOMO-1→LUMO and HOMO-1→LUMO+1 with oscillator strengths $f = 0.03-0.12$. The energy diagram of the FMOs and respective isosurfaces are shown Fig.5. An analysis of atomic composition of these FMOs responsible for the experimentally observed absorption band indicate that all of them HOMO and HOMO-1 as well as LUMO and LUMO+1 are dominantly localized (up to 85-90 %)

at the iminomethylphenyl (**ImPh**) fragments of the two ligands within the complex (Fig.5). As one can see, HOMO and HOMO-1 are of the bonding π character and the respective electronic density is delocalized between the two ligands. Meanwhile, LUMO and LUMO+1 are of the antibonding π^* character but the electron density is localized at either of the two ligands separately. There is also a minor contribution of charge transfer from the tosyl (**Ts**) and hydroxyalkyl (**HydAlk**) fragments. Thus, the experimentally observed band of UV-vis spectra at 353 nm is due to a superposition of $\pi \rightarrow \pi^*$ electronic transitions with a dominant ligand-to-ligand charge transfer (LLCT) character. The same interpretation of UV-vis spectra was obtained for all other zinc complexes (Table S1-S5, Fig. S1-S5).

Table 3.

Figure 5.

3.5. *Biological activity of the azomethines and zinc complexes*

The protistocidal, antibacterial, and fungistatic activities of the azomethines **1a-e** and zinc complexes **2a-e** made here were studied. The test results are presented in Table 4.

Table 4.

As it can be judged from Table 4, most promising results relate to the protistocidal and bacteriostatic properties. The azomethines **1a-e** have been shown to have only protistocidal activity. Compounds **1a,c-e** have the same activity as toltrazuril, but azomethine **1b** was twice less active than the commercial drug.

The some complexes **2** show a very high protistocidal activity against *Colpoda steinii*. More specifically, the complex **2a** is four times more active than the commercial drug toltrazuril taken as a reference, and the complex **2d** is nearly as active as toltrazuril. The complexes **2a-e** also show a pronounced bacteriostatic

activity against *Staphylococcus aureus* with the complex **2e** being twice more active than the commercial drug sulfadimethoxine taken as a reference.

Two out of five compounds of the series also demonstrate a fungistatic activity against *Penicillium italicum*, however, it does not exceed that of the commercial drug fundazol.

Therefore, some members of the zinc complexes with N-[2-(hydroxyalkyliminomethyl)phenyl]-4-methylbenzenesulfonamide ligands show higher fungistatic and protistocidal activities exceeding those of approved free ligands and commercial drugs, which encourages the further search for compounds with medicine-important bioactivity among this family.

Acknowledgements

The work was performed with the financial support of the Ministry of Education and Science of the Russian Federation (the State assignment: project 4.5388.2017/8.9). IR, UV-vis, PL, PLE, and ^1H NMR spectra were measured using equipment of the center for collective use "Molecular spectroscopy" at the SFU. X-ray absorption spectra were measured at the Unique Scientific Facility Kurchatov Synchrotron Radiation Source funded by the Ministry of education and science of the Russian Federation (project RFMEFI61914X0002).

References

- [1] Z.H. Chohan, M. Arif, N. Sarfraz, *Appl. Organomet. Chem.* 21 (2007) 294.
- [2] M.T. Kaczmarek, R. Jastrza, E. Holderna-Kedzia, V. Radetzky-Paryzek, *Inorg. Chim. Acta.* 362 (2009) 3127.
- [3] Q. Huang, Z.Q. Pan, P. Wang, Z.P. Chen, X.L. Zhang, H.S. Xu, *Bioorg. Med. Chem. Lett.* 16 (2006) 3030.
- [4] M.C. Rodríguez-Argüelles, M. Ferrari Belichi, F. Bisceglie, C. Pelizzi, G. Pelosi, S. Pinelli, M. Sassi, *J. Inorg. Biochem.* 98 (2004) 313.
- [5] H. Zhang, C.S. Liu, X.H. Bu, M. Yang, *J. Inorg. Biochem.* 99 (2005) 1119.
- [6] Z. Trávníček, V. Kryštof, M. Šipl, *J. Inorg. Biochem.* 100 (2006) 214.
- [7] X. Sheng, X. Guo, M.X. Lu, Y.G. Lu, Y. Shao, F. Liu, Q. Xu, *Bioconjugate Chem.* 19 (2008) 490.
- [8] J. Tang, B. Wang, L. Zhu, *Bioorg. Med. Chem.* 17 (2009) 614.
- [9] Q. Jiang, J. Zhu, Y. Zhang, N. Xiao, Z. Guo, *Biometal.* 22 (2009) 297.
- [10] A. Nakayama, M. Hiromura, Y. Adachi, H. Sakurai, *J. Biol. Inorg. Chem. (JBIC)* 13 (2008) 675.
- [11] H. Sakurai, Y. Yoshikawa, H. Yasui, *Chem. Soc. Rev.* 37 (2008) 2383.
- [12] B. Naskar, R. Modak, J. Sikdar, D.K. Maiti, A. Banik, T.K. Dangar, S. Mukhopadhyay, D. Mandal, S. Goswami, *J. Photochem. Photobiol. Chem.* 321 (2016) 99.
- [13] V.A. Lazarenko, P.V. Dorovatovskii, Y.V. Zubavichus, A.S. Burlov, Y.V. Koshchienko, V.G. Vlasenko, V.N. Khrustalev, *Crystals* 7 (2017) 325.
- [14] T. Akimoto, M. Maeda, A. Tsuji, Y. Iitaka, *Chem. Pharmacy. Bull.* 27 (1979) 424.
- [15] M. Dey, C.P. Rao, P. Saarenketo, K. Rissanen, E. Kolehmainen, *Eur. J. Inorg. Chem.* (2002) 2207.
- [16] A.V. Pestov, P.A. Slepukhin, V.N. Charushin, *Russ. Chem. Rev.* 84 (2015) 310.

- [17] V.A. Kogan, V.V. Zelentsov, O.A. Osipov, A.S. Burlov, *Russ. Chem. Rev.* 48 (1979) 645.
- [18] A.S. Burlov, S.A. Nikolaevskii, Yu.V. Koshchienko, A.I. Uraev, I.S. Vasilchenko, G.S. Borodkin, A.D. Garnovskii, V.N. Ikorskii, V.G. Vlasenko, Ya.V. Zubavichus, D.A. Garnovskii, *Russ. J. Inorg. Chem.* 53 (2008) 1566.
- [19] A.S. Burlov, A.I. Uraev, S.A. Nikolaevskii, Yu.V. Koshchienko, I.S. Vasilchenko, L.N. Divaeva, G.S. Borodkin, A.D. Garnovskii, V.N. Ikorskii, D.A. Garnovskii, V.G. Vlasenko, Ya.V. Zubavichus, *Russ. J. Gen. Chem.* 78 (2008) 1230.
- [20] A.S. Burlov, Yu.V. Koshchienko, A.I. Uraev, I.S. Vasilchenko, D.A. Garnovskii, G.S. Borodkin, S.A. Nikolaevskii, A.D. Garnovskii, V.N. Ikorskii, V.G. Vlasenko, I.A. Zarubin, *Russ. J. Inorg. Chem.* 51 (2006) 1065.
- [21] T. Sano, Y. Nishio, Y. Hamada, H. Takahashi, T. Usuki, K. Shibata, *J. Mater. Chem.* 10 (2000) 157.
- [22] A.S. Burlov, V.G. Vlasenko, D.A. Garnovskii, A.I. Uraev, E.I. Mal'tsev, D.A. Lypenko, A.V. Vannikov. *Electroluminescent organic light-emitting diodes based on coordination compounds*. Rostov-on-Don: S.F.U., 2015. 228 p.
- [23] A.S. Burlov, E.I. Mal'tsev, V.G. Vlasenko, D.A. Garnovskii, A.V. Dmitriev, D.A. Lypenko, A.V. Vannikov, P.V. Dorovatovskii, V.A. Lazarenko, Y.V. Zubavichus, V.N. Khrustalev, *Polyhedron*. 133 (2017) 231.
- [24] T.P. Lysakova, A.S. Burlov, V.G. Vlasenko, Yu.V. Koshchienko, G.G. Aleksandrov, S.I. Levchenkov, Y.V., Zubavichus, S.A. Cheprasov, D.A. Garnovskii, A.V. Metelitsa., *Russ. J. Coord. Chem.* 42 (2016) 674.
- [25] A.S. Burlov, V.G. Vlasenko, N.I. Makarova, K.A. Lysenko, V.V. Chesnokov, G.S. Borodkin, I.S. Vasilchenko, A.I. Uraev, A.D. Garnovskii, A.V. Metelitsa, *Polyhedron*. 107 (2016) 153.
- [26] A.S. Burlov, Yu.V. Koshchienko, N.I. Makarova, T.A. Kuz'menko, V.V. Chesnokov, M.A. Kiskin, S.A. Nikolaevskii, D.A. Garnovskii, A.I. Uraev, V.G. Vlasenko, A.V. Metelitsa, *Synth. Met.* 220 (2016) 543.

- [27] Yu.V. Koshchienko, A.S. Burlov, N.I. Makarova, V.G. Vlasenko, S.A. Nikolaevskii, A.S. Kiskin, G.G. Alexandrov, D.A. Garnovskii, A.V. Metelitsa, V.I. Minkin, *Russ. J. Gen. Chem.* 87 (2017) 80.
- [28] S. Parker, *Photoluminescence of Solutions*, Mir, Moskow (1972), 247 p.
- [29] S. R. Meech, D. Phillips, *J. Photochem.* 23 (1983) 193.
- [30] A.A. Chernyshov, A.A. Veligzhanin, Y.V. Zubavichus, *Nucl. Instr. Meth. Phys. Res. A.* 603 (2009) 95.
- [31] B. Ravel, M. Newville, *J. Synchrotron Rad.* 12 (2005) 537.
- [32] S.I. Zabinski, J.J. Rehr, A. Ankudinov, R.C. Albers, M. Eller, *J. Phys. Rev. B.* 52 (1995) 2995.
- [33] M.J. Frisch, G.W. Trucks, H.B. Schlegel, G.E. Scuseria, M.A. Robb, J.R. Cheeseman, J.A. Montgomery, Jr. T. Vreven, K.N. Kudin, J.C. Burant, J.M. Millam, S.S. Iyengar, J. Tomasi, V. Barone, B. Mennucci, M. Cossi, G. Scalmani, N. Rega, G.A. Petersson, H. Nakatsuji, M. Hada, M. Ehara, K. Toyota, R. Fukuda, J. Hasegawa, M. Ishida, T. Nakajima, Y. Honda, O. Kitao, H. Nakai, M. Klene, X. Li, J.E. Knox, H.P. Hratchian, J.B. Cross, V. Bakken, C. Adamo, J. Jaramillo, R. Gomperts, R.E. Stratmann, O. Yazyev, A.J. Austin, R. Cammi, C. Pomelli, J.W. Ochterski, P.Y. Ayala, K. Morokuma, G.A. Voth, P. Salvador, J.J. Dannenberg, V.G. Zakrzewski, S. Dapprich, A.D. Daniels, M.C. Strain, O. Farkas, D.K. Malick, A.D. Rabuck, K. Raghavachari, J.B. Foresman, J.V. Ortiz, Q. Cui Piskorz, I. Komaromi, R.L. Martin, D.J. Fox, T. Keith, M.A. Al-Laham, C.Y. Peng, A. Nanayakkara, M. Challacombe, P.M.W. Gill, B. Johnson, W. Chen, M.W. Wong, C. Gonzalez, J.A. Pople, *Gaussian 03, Revision A.1*, Gaussian, Inc., Pittsburgh PA, USA (2003).
- [34] A.D. Becke, *J. Chem. Phys.* 98 (1993) 5648.
- [35] C. Lee, W. Yang, R.G. Parr, *Phys. Rev.* 37 (1988) 785.
- [36] G.A. Petersson, A. Bennett, T.G. Tensfeldt, M.A. Allaham, W.A. Shirley, J. Mantzaris, *J. Chem. Phys.* 89 (1988) 2193.
- [37] R. Ditchfield, W.J. Hehre, J.A. Pople, *J. Chem. Phys.* 54 (1971) 724.
- [38] J. Tomasi, B. Mennucci, R. Cammi, *Chem. Rev.* 105 (2005) 2999.

- [39] Determination of the Sensitivity of Microorganisms to Antibacterial Drugs: Guidelines. MUK 4.2.1890-04, Moscow: Medicine, 2004.
- [40] G.N. Pershin, Methods of Experimental Chemotherapy, Moscow: Medicine, 1971, p. 100.
- [41] L.N. Fetisov, A.A. Zubenko, A.N. Bodryakov, M.A. Bodryakova, Proc. Int. Parasitol. Symp. "Modern Problems of General and Partial Parasitology" (2012) 70.
- [42] Manual on Experimental (Preclinical) Study of New Pharmaceuticals, Khabriev, R.U., Ed., Moscow: Medicine, 2005.
- [43] A.S. Burlov, A.I. Uraev, D.A. Garnovskii, K.A. Lyssenko, V.G. Vlasenko, Y.V. Zubavichus, V.Yu. Murzin, E.V. Korshunova, G.S. Borodkin, S.I. Levchenkov, I.S. Vasilchenko, V.I. Minkin, J. Mol. Struct. 1064 (2014) 111.
- [44] P. Zabierowski, J. Szklarzewicz, K. Kurpiewska, K. Lewiński, W. Nitek, Polyhedron 49 (2013) 74.
- [45] P. Bhowmik, N. Aliaga-Alcalde, V. Gómez, M. Corbella, S. Chattopadhyay, Polyhedron 49 (2013) 269.
- [46] J. Sanmartín, F. Novio, A.M. García-Deibe, M. Fondo, N. Ocampo, M.R. Bermejo, Eur. J. Inorg. Chem. (2008) 1719.
- [47] R. Pedrido, M.R. Bermejo, A.M. García-Deibe, A.M. González-Noya, M. Maneiro, M. Vázquez, Eur. J. Inorg. Chem. (2003) 3193.
- [48] V.G. Vlasenko, D.A. Garnovskii, G.G. Aleksandrov, N.I. Makarova, S.I. Levchenkov, Ya.V. Zubavichus, A.I. Uraev, Yu.V. Koshchienko, A.S. Burlov, Polyhedron.133 (2017) 245.
- [49] Yu.V. Koshchienko, A.S. Burlov, N.I. Makarova, V.G. Vlasenko, S.A. Nikolaevskii, M.A. Kiskin, D.A. Garnovskii, A.L. Trigub, A.V. Metelitsa, Russ. J. Gen. Chem. 87 (2017) 764.
- [50] A.S. Burlov, V.G. Vlasenko, A.V. Dmitriev, V.V. Chesnokov, A.I. Uraev, D.A. Garnovskii, Y.V. Zubavichus, A.L. Trigub, I.S. Vasilchenko, D.A. Lypenko, E.I. Mal'tsev, T.V. Lifintseva, G.S. Borodkin, Synth. Metals. 203 (2015) 156.

Table 1. Parameters of the local structure around zinc ions in complexes **2a-e**: coordination numbers (N), interatomic distances (R), and Debye-Waller factors (σ^2). Q is the integral fit quality factor.

Sample	N	R, Å	σ^2 , Å ²	CS	Q, %
2a	4	2.02	0.0035	N	1.5
2b	4	2.03	0.0035	N	1.7
2c	4	2.03	0.0032	N	2.2
2d	4	2.02	0.0031	N	2.4
2e	4	2.03	0.0032	N	1.5

Table 2. UV-vis and photoluminescence characteristics of **2a-e** in DMSO at 293 K:
 ε - molar extinction coefficient; ϕ - quantum yield of fluorescence.

Compound	Absorption λ_{\max} , nm (ε , M ⁻¹ cm ⁻¹)	Photoluminescence		
		Excitation λ_{\max} , nm	Emission λ_{\max} , nm	ϕ
2a	353 (11540)	350	430	0.32
	270 (23700)			
2b	353 (12320)	350	430	0.34
	270 (25300)			
2c	353 (12890)	350	430	0.35
	270 (25100)			
2d	353 (12340)	350	429	0.35
	270 (21700)			
2e	353 (12680)	350	428	0.32
	270 (25280)			

Table 3. Calculated wavelengths (λ), energies (E), oscillator strengths (f), involved molecular orbitals and their contributions for different electronic transitions in **2a** according to TD-DFT calculations.

λ_{cal} , nm	E, eV	Electronic transitions, (contribution, %)	f	Character
364.54	3.4012	HOMO \rightarrow LUMO (90 %)	0.081	$\pi \rightarrow \pi^*$
352.66 (353) [†]	3.5157	HOMO \rightarrow LUMO+1 (83)	0.117	$\pi \rightarrow \pi^*$
345.65	3.5870	HOMO-1 \rightarrow LUMO (86)	0.047	$\pi \rightarrow \pi^*$
333.33	3.7195	HOMO-1 \rightarrow LUMO+1 (90)	0.031	$\pi \rightarrow \pi^*$
292.09	4.2448	HOMO-1 \rightarrow LUMO+3 (11) HOMO \rightarrow LUMO+2 (77)	0.0001	$\pi \rightarrow \pi^*$
290.27	4.2713	HOMO-1 \rightarrow LUMO+2 (18) HOMO \rightarrow LUMO+3 (71)	0.0247	$\pi \rightarrow \pi^*$

[†] experimental value

Table 4. Fungistatic, protistocidal, and bacteriostatic activities of the free ligands (**1a-e**) and zinc complexes (**2a-e**) in a comparison with relevant commercial drugs.

Compound	<i>Penicillium italicum</i> , inhibition zone diameter, mm	<i>Colpoda steinii</i> , $\mu\text{g/mL}$	<i>Escherichia coli</i> 078, $\mu\text{g/mL}$	<i>Staphylococcus</i> <i>aureus</i> P-209, $\mu\text{g/mL}$
1a	0	62.5	>500	>500
1b	0	125	>500	>500
1c	0	62.5	>500	>500
1d	0	62.5	>500	>500
1e	0	62.5	>500	>500
2a	8.0	15.6	>500	250
2b	0	125	>500	500
2c	0	500	>500	>500
2d	0	62.5	>500	125
2e	10	250	>500	31.25
Sulfadime- thoxine	-	-	62.5	62.5
Toltrazuril	-	62.5	-	-
Fundazol	22	-	-	-

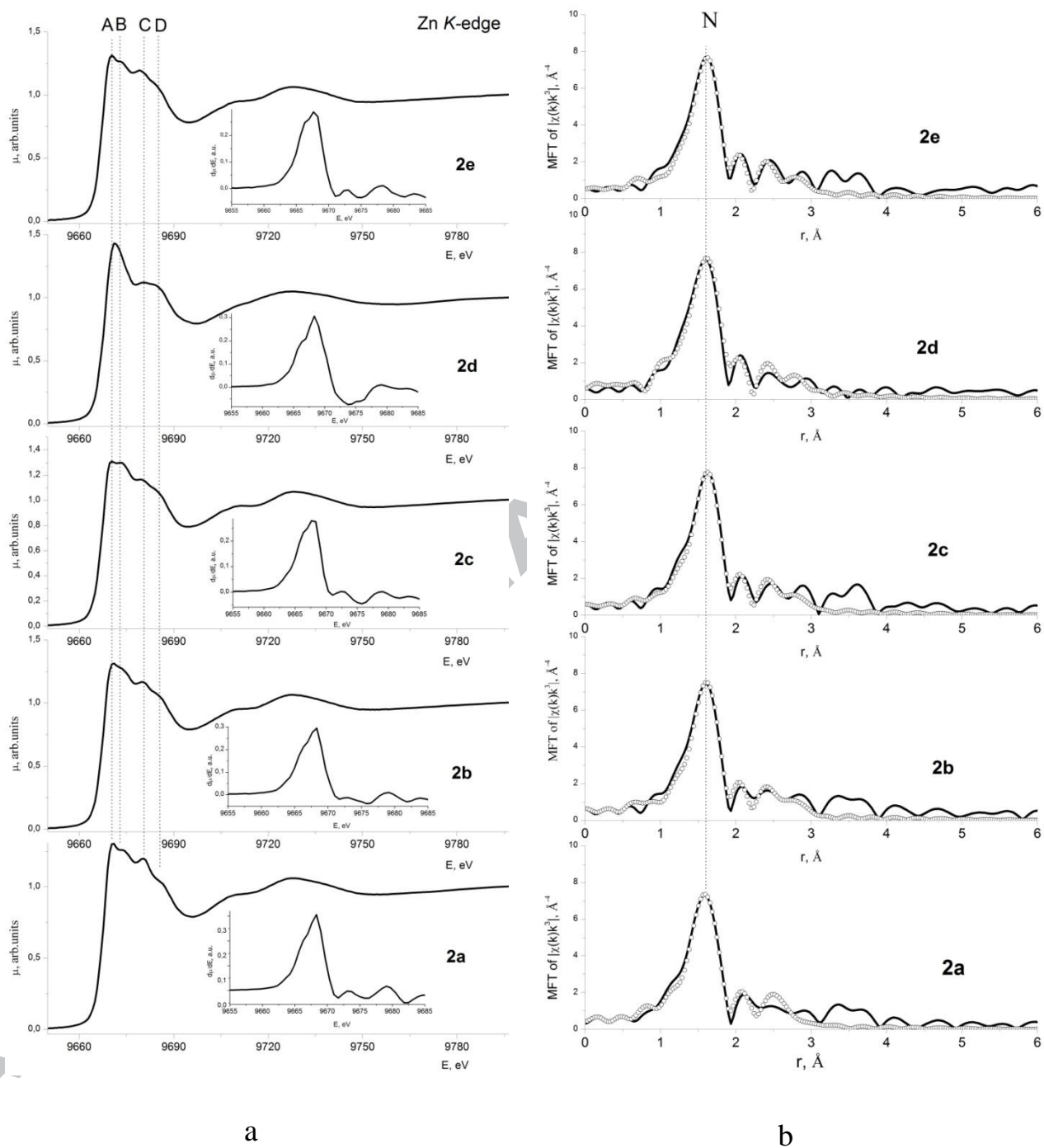


Fig. 1. Zn K-edge XANES spectra for the zinc complexes **2a-e** (a) represented as $\mu(E)$ and $d\mu/dE$ (insets), MFT EXAFS $\chi(k)k^3$ for zinc complexes **2a-e**, experiment - solid line, best-fit theory - empty circles (b).

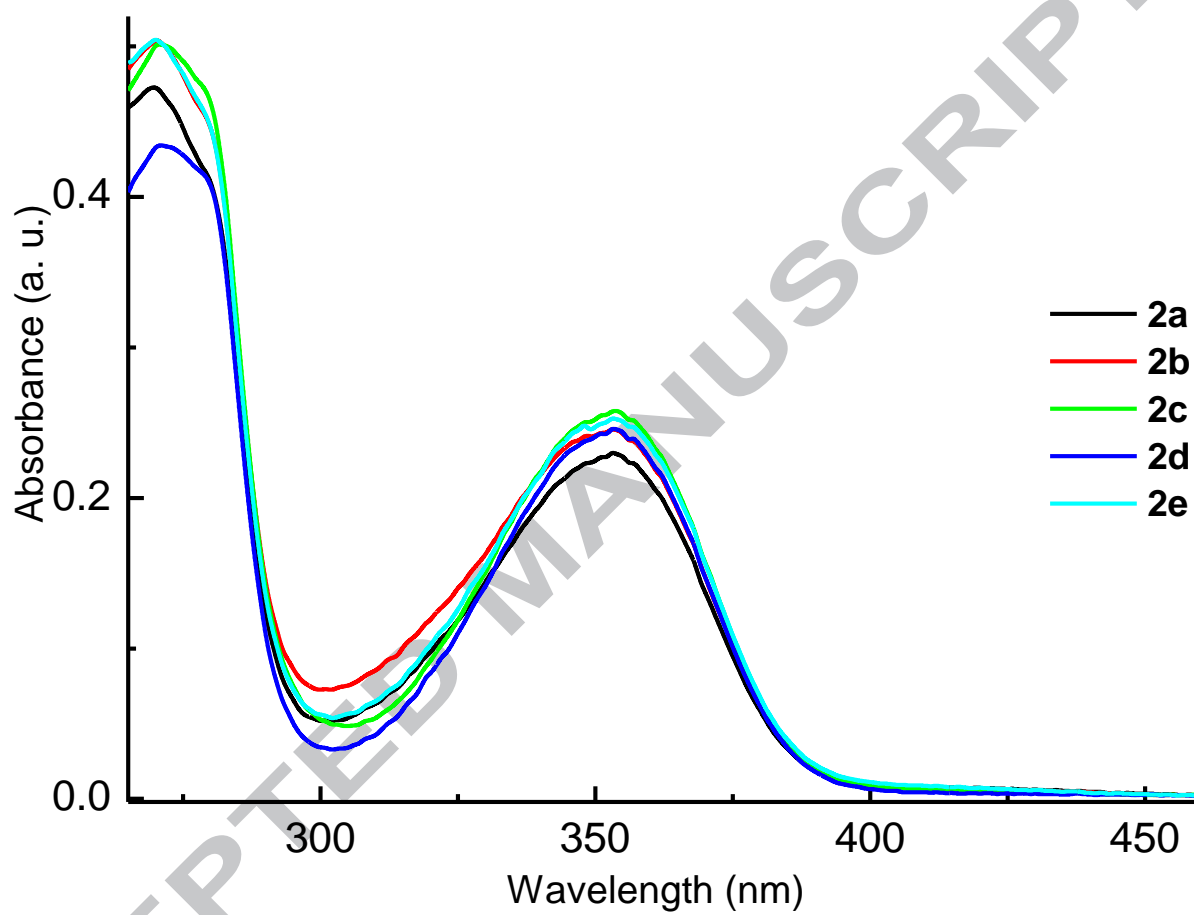


Fig. 2. UV-vis spectra of compounds **2a-e** in DMSO.

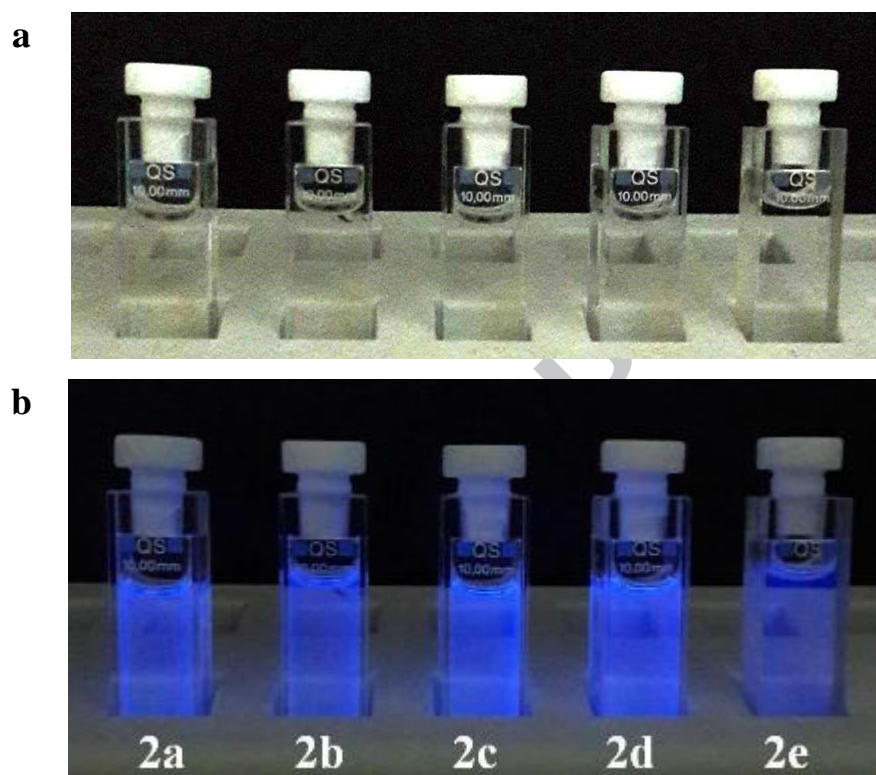


Fig. 3. Solutions photographs of compounds **2a-e** in DMSO: a) before radiation (no emission); b) during radiation (emission, $\lambda_{\text{ex}} = 365 \text{ nm}$) at room temperature.

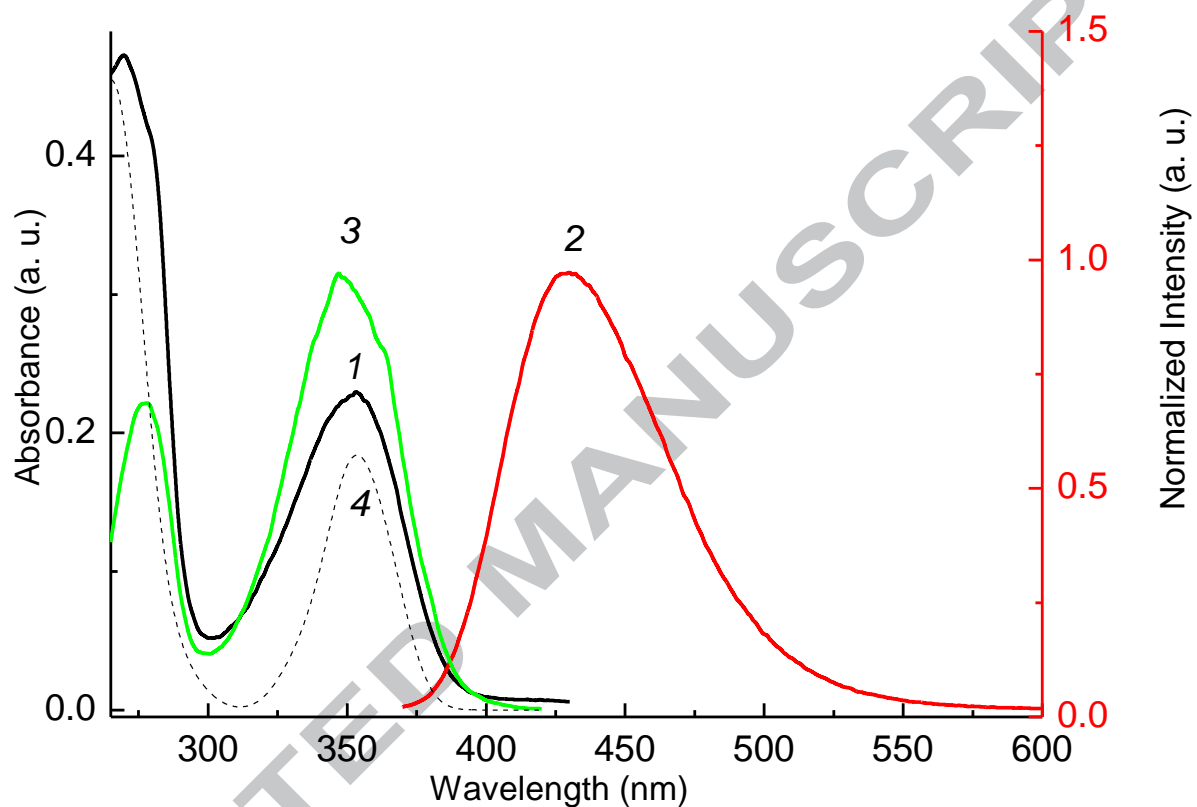


Fig. 4. UV-vis (1), fluorescence emission ($\lambda_{\text{ex}} = 350$ nm) (2) and fluorescence excitation ($\lambda_{\text{obs}} = 430$ nm) (3) spectra of **2a** in DMSO. The dotted line (4) shows a theoretically calculated UV-vis spectrum.

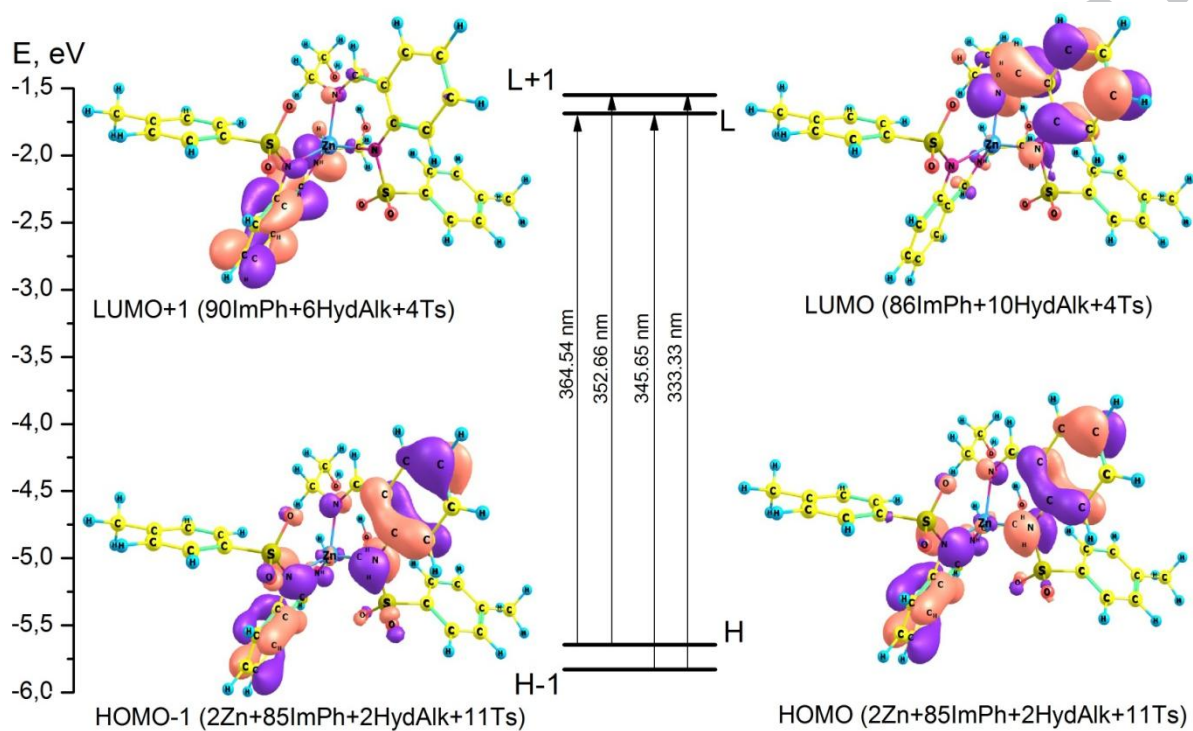


Fig. 5. The energy level diagram and isosurfaces of the frontier molecular orbitals for **2a** and wavelengths of derived electronic transitions.

HIGHLIGHTS

- A new series of Zn(II) complexes were prepared with Schiff bases ligand derived by condensation of 2-tosylammonobenzaldehyde with various aminoalcohols.
- *The local atomic structure* around Zn atoms in complexes was determined by EXAFS.
- The electronic absorption spectra, photoluminescence, and biological activities of the complexes were investigated.

